Pentaquarks at LHCb

Nathan Jurik

Syracuse University

On behalf of the LHCb Collaboration

Tetra- and Penta-quarks conceived at the birth of Quark Model

Volume 8, number 3 PHYSICS LETTERS 1 February 1964

A SCHEMATIC MODEL OF BARYONS AND MESONS *

M. GELL-MANN
California Institute of Technology, Pasadena, California

Received 4 January 1964

...

A simpler and more elegant scheme can be constructed if we allow non-integral values for the charges. We can dispense entirely with the basic baryon b if we assign to the triplet t the following properties: spin $\frac{1}{2}$, $z = -\frac{1}{3}$, and baryon number $\frac{1}{3}$. We then refer to the members $u^{\frac{2}{3}}$, $d^{-\frac{1}{3}}$, and $s^{-\frac{1}{3}}$ of the triplet as "quarks" 6) q and the members of the anti-triplet as anti-quarks $\bar{q}$. Baryons can now be constructed from quarks by using the combinations (qqq), $(qqqq\bar{q})$, etc., while mesons are made out of $(q\bar{q})$, $(qq\bar{q}\bar{q})$, etc. It is assuming that the lowest baryon configuration (qqq) gives just the representations **1**, **8**, and **10** that have been observed, while

8419/TH.412
21 February 1964

AN SU_3 MODEL FOR STRONG INTERACTION SYMMETRY AND ITS BREAKING
II *)

G. Zweig
CERN---Geneva

*) Version I is CERN preprint 8182/TH.401, Jan. 17, 1964.

...

6) In general, we would expect that baryons are built not only from the product of three aces, AAA, but also from $\bar{A}AAAA$, $\bar{A}\bar{A}AAAA$, etc., where $\bar{A}$ denotes an anti-ace. Similarly, mesons could be formed from $\bar{A}A$, $\bar{A}\bar{A}AA$ etc. For the low mass mesons and baryons we will assume the simplest possibilities, $\bar{A}A$ and AAA, that is, "deuces and treys".

- Searches for such states made out of the light quarks (u,d,s) are ~50 years old, but no undisputed experimental evidence have been found for them
- However several charmonium and bottomonium-like tetraquark candidates have been observed

$\Lambda_b^0 \rightarrow J/\psi\ p\ K^-$ At LHCb

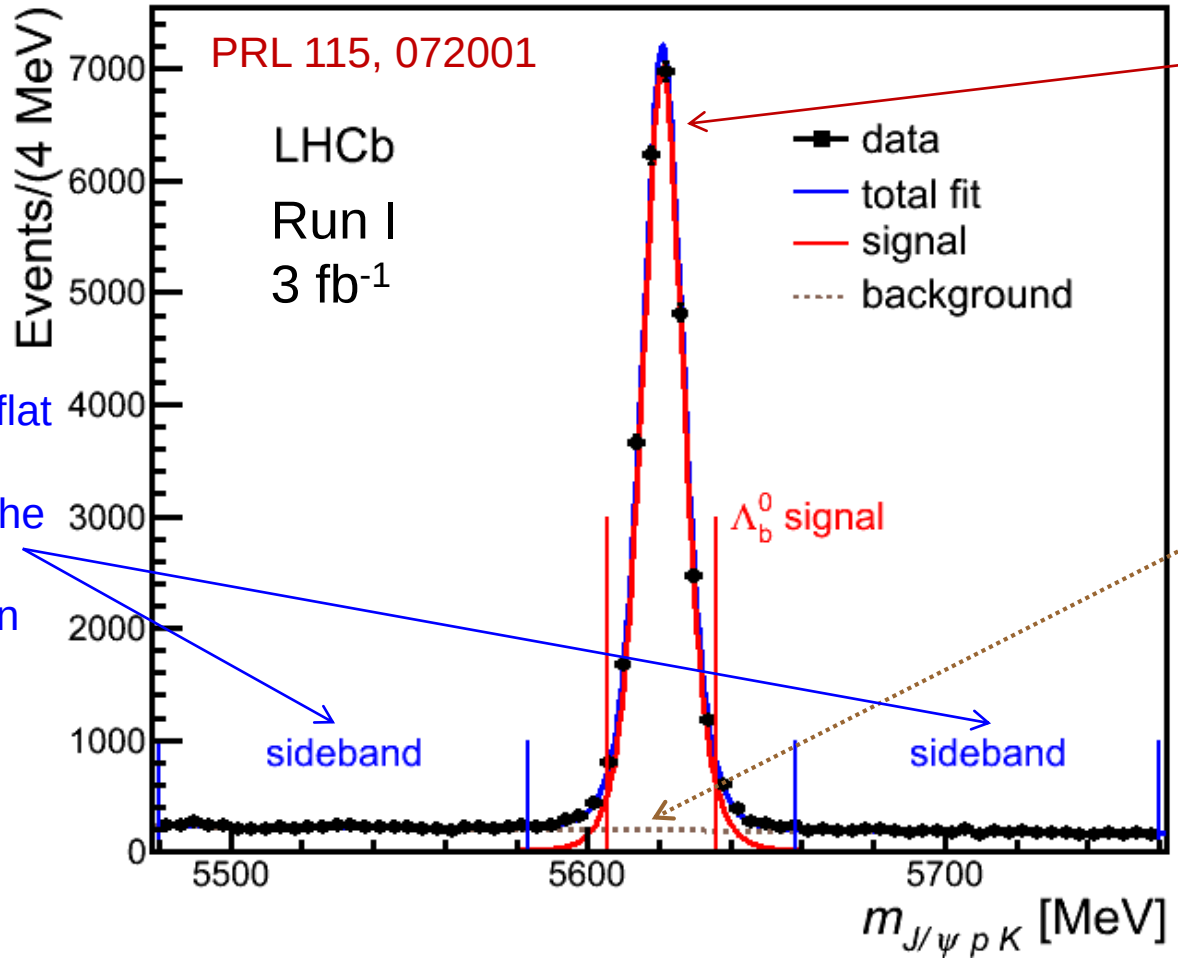

26,007±166 Λ_b^0 candidates

The sideband distributions are flat → no major reflections from the other b-hadrons after the selection

The background is only 5.4% in the signal region!

- The decay first observed by LHCb and used to measure Λ_b^0 lifetime PRL 111, 102003 (2013)

An unexpected structure in $m_{J/\psi p}$

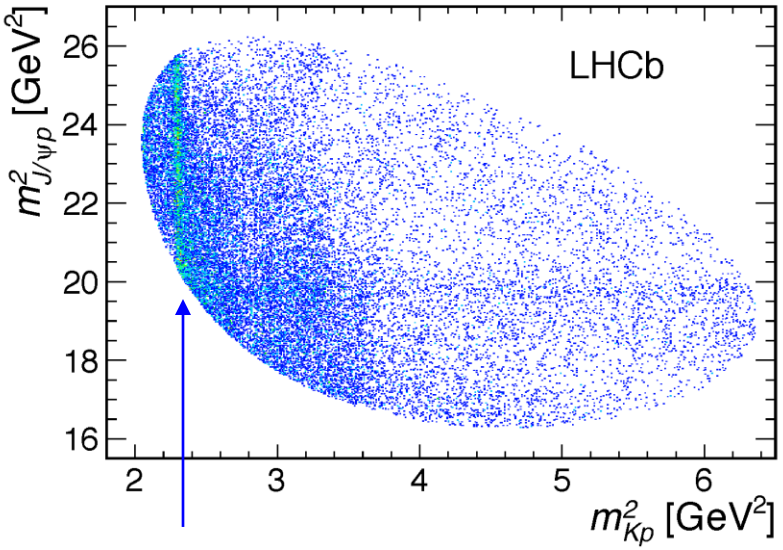

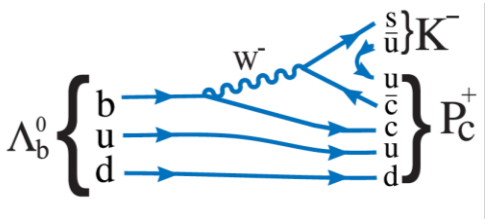

$P_c^+ \rightarrow J/\psi\ p$?

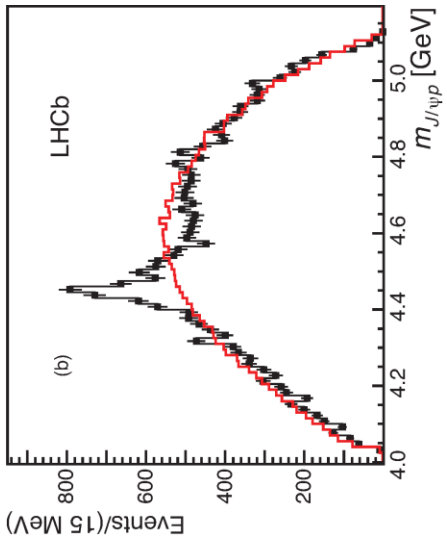

$\Lambda(1520)$ and other Λ^*'s $\rightarrow$ p K$^-$

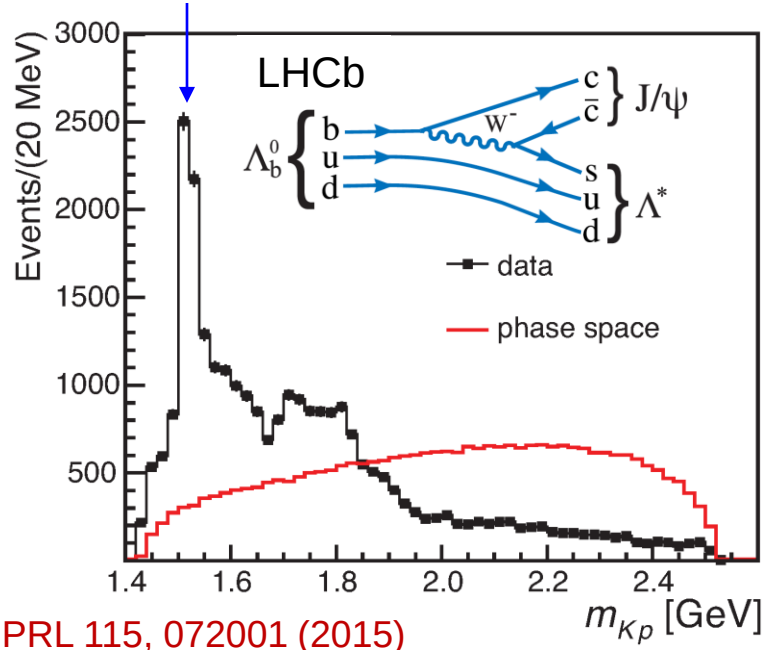

PRL 115, 072001 (2015)

Unexpected narrow peak in $m_{J/\psi p}$!

Necessary Checks

- Many checks done to ensure it is not an “artifact” of selection:
  - Efficiency across Dalitz plane is smooth, wouldn’t create peaking structures.

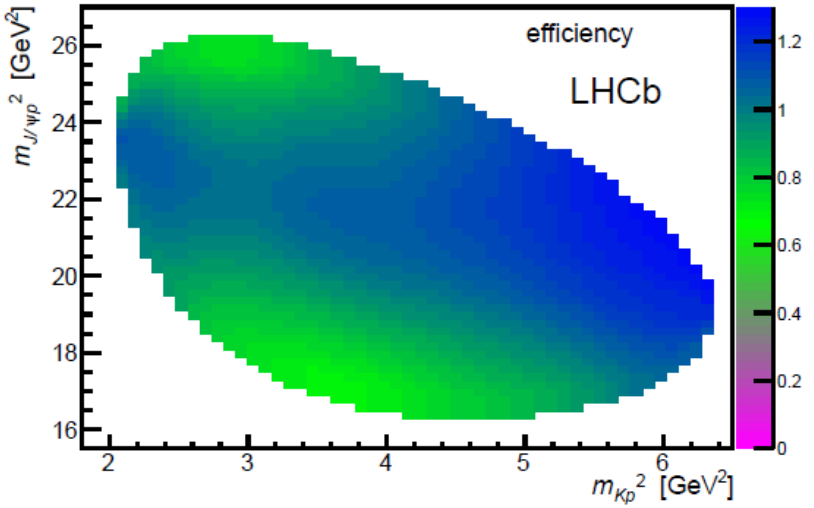

  - The same P_c^+ structure found using very different selections by different LHCb teams
  - Suppress fake tracks
  - Split data shows consistency: 2011/2012, magnet up/down, $\Lambda_b/\overline{\Lambda}_b$, Λ_b(p_T low)/Λ_b(p_T high)
  - Veto $B_s \to J/\psi K^- K^+$ & $B^0 \to J/\psi K^- \pi^+$ decays
  - Exclude Ξ_b or other high mass decays as a possible source

Amplitude Analysis of $\Lambda_b^0 \to J/\psi p K^-$, $J/\psi \to \mu^+\mu^-$

- Could it be a reflection of interfering Λ^*'s $\to$ p K^- ?
  - Full amplitude analysis absolutely necessary!
- Analyze all dimensions of the decay kinematics for $\Lambda_b^0 \to J/\psi p K^-$, $J/\psi \to \mu^+\mu^-$.

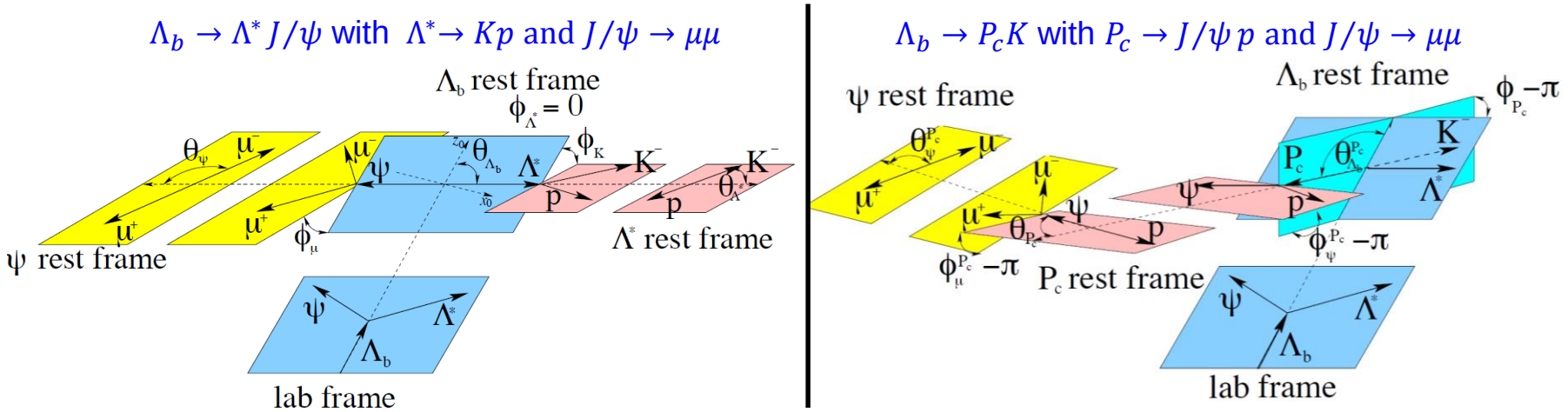

- Write down (6D) matrix element with helicity formalism and allow the two decay chains to interfere:

$$|\mathcal{M}|^2 = \sum_{\lambda_{\Lambda_b^0}} \sum_{\lambda_p} \sum_{\Delta\lambda_\mu} \left| \mathcal{M}^{\Lambda^*}_{\lambda_{\Lambda_b^0}, \lambda_p, \Delta\lambda_\mu} + e^{i\,\Delta\lambda_\mu \alpha_\mu} \sum_{\lambda_p^{P_c}} d^{\frac{1}{2}}_{\lambda_p^{P_c}, \lambda_p}(\theta_p)\, \mathcal{M}^{P_c}_{\lambda_{\Lambda_b^0}, \lambda_p^{P_c}, \Delta\lambda_\mu} \right|^2$$

Λ^* resonance model

- Large number of possibly contributing resonances, each contributing 4-6 complex helicity couplings which need to be determined by the data.
- We use two models in our fits to study the dependence on Λ^* model.

State	J^P	M_0 (MeV)	Γ_0 (MeV)	# Reduced amplitudes	# Extended amplitudes
$\Lambda(1405)$	$1/2^-$	$1405.1^{+1.3}_{-1.0}$	50.5 ± 2.0	3	4
$\Lambda(1520)$	$3/2^-$	1519.5 ± 1.0	15.6 ± 1.0	5	6
$\Lambda(1600)$	$1/2^+$	1600	150	3	4
$\Lambda(1670)$	$1/2^-$	1670	35	3	4
$\Lambda(1690)$	$3/2^-$	1690	60	5	6
$\Lambda(1800)$	$1/2^-$	1800	300	4	4
$\Lambda(1810)$	$1/2^+$	1810	150	3	4
$\Lambda(1820)$	$5/2^+$	1820	80	1	6
$\Lambda(1830)$	$5/2^-$	1830	95	1	6
$\Lambda(1890)$	$3/2^+$	1890	100	3	6
$\Lambda(2100)$	$7/2^-$	2100	200	1	6
$\Lambda(2110)$	$5/2^+$	2110	200	1	6
$\Lambda(2350)$	$9/2^+$	2350	150	0	6
$\Lambda(2585)$	$5/2^-$?	$\approx$2585	200	0	6
		Total fit parameters:		64	146

Fit with $\Lambda^* \to pK^-$ contributions only

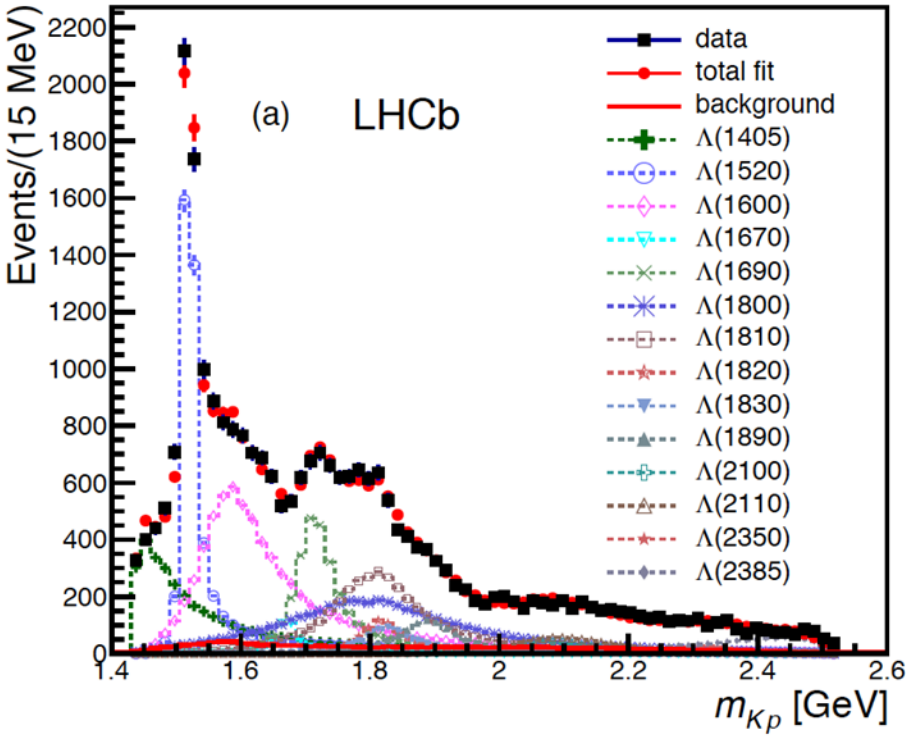

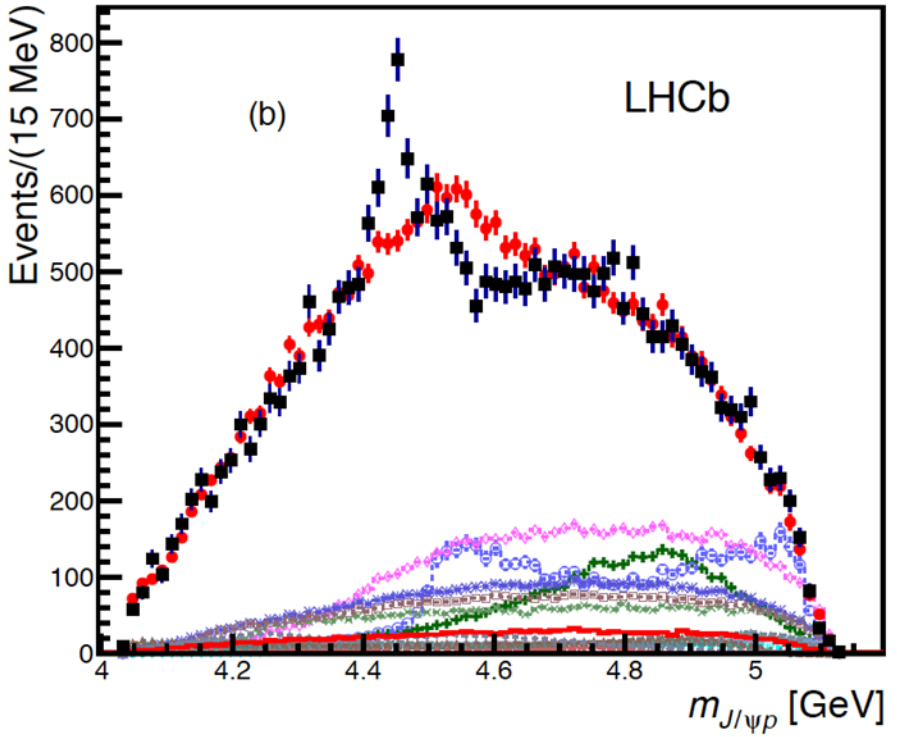

- m_{Kp} looks fine, but $m_{J/\psi p}$ looks terrible
- Addition of non-resonant terms, Σ^*'s or extra Λ^*'s doesn't help.
- There is no ability to describe the peaking structure with conventional resonances!

Fit with Λ^*'s and one $P_c^+ \rightarrow J/\psi p$ state

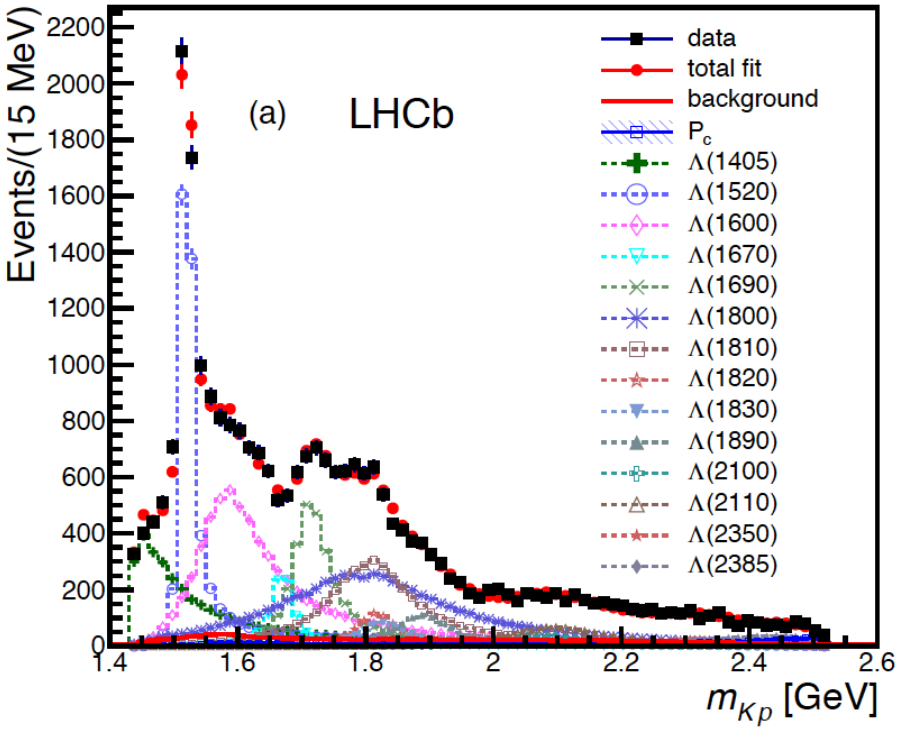

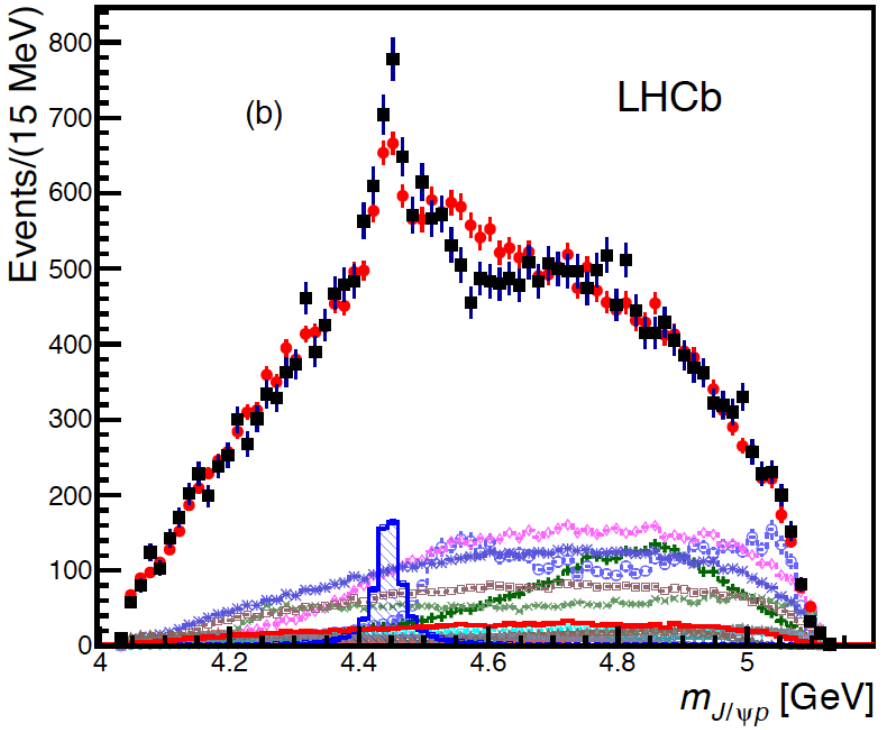

(extended Λ^* model)

- Try all J^P of P_c^+ up to $7/2^{\pm}$ and best fit has $J^P = 5/2^{\pm}$.
- Still not a good fit though, evidently something further is needed.

Fit with Λ^*'s and two $P_c^+ \to J/\psi p$ states

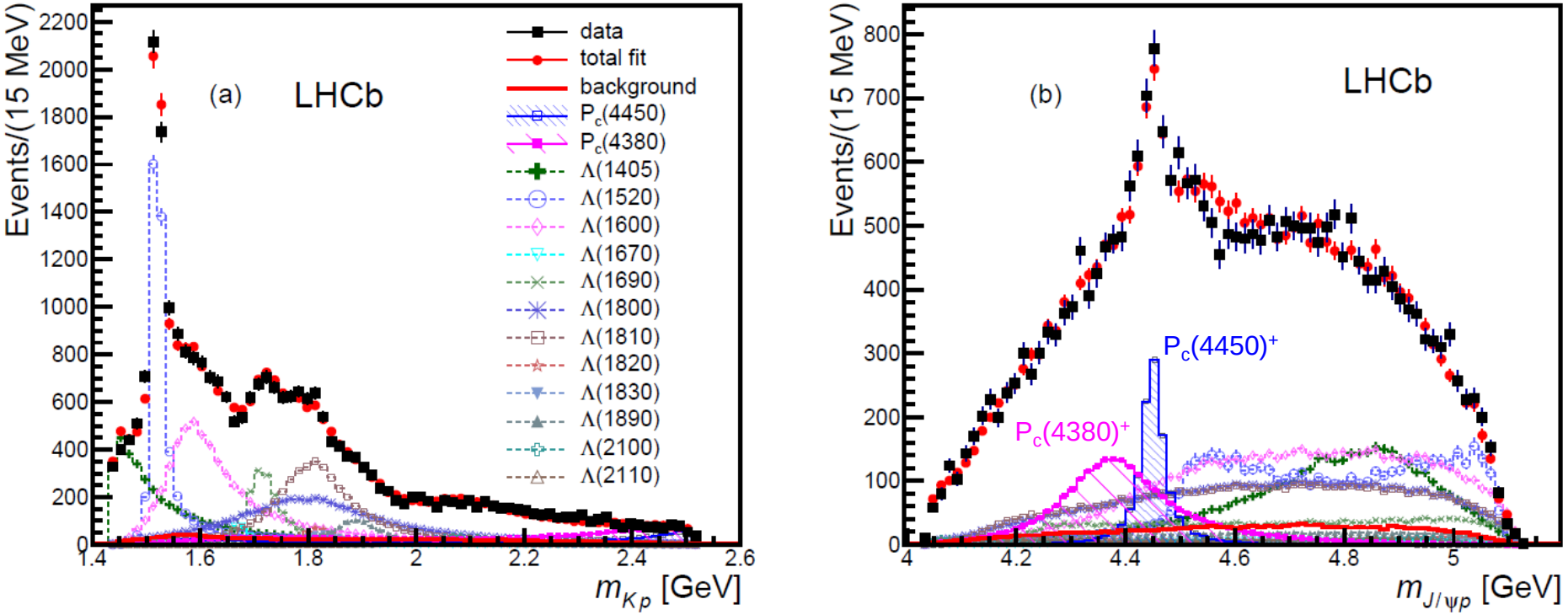

(reduced Λ^* model)

- With two P_c resonances we are able to describe the peaking structure!
- Obtain good fits even with the reduced Λ^* model
- Best fit has $J^P(P_c(4380), P_c(4450))$=(3/2$^-$, 5/2$^+$), also (3/2$^+$, 5/2$^-$) and (5/2$^+$, 3/2$^-$) are preferred

Angular distributions

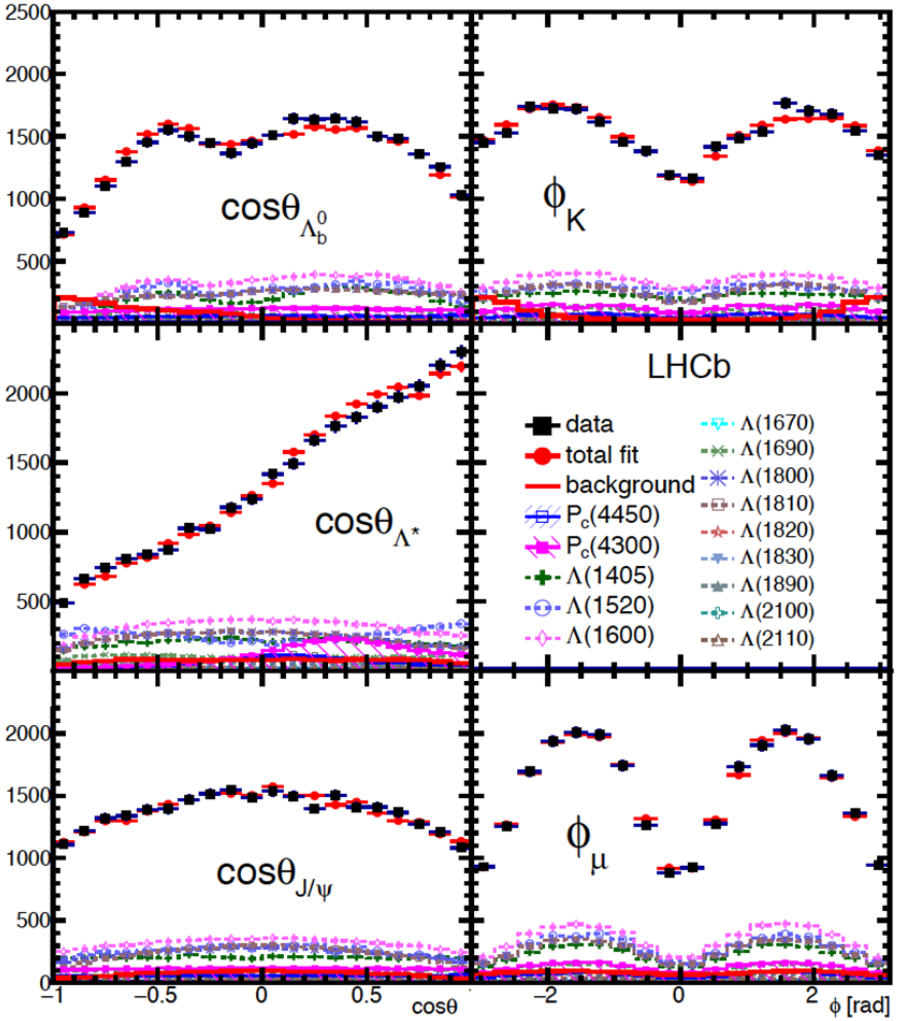

- Good description of the data in angular distributions too!

Data preference for opposite parity P_c^+ states

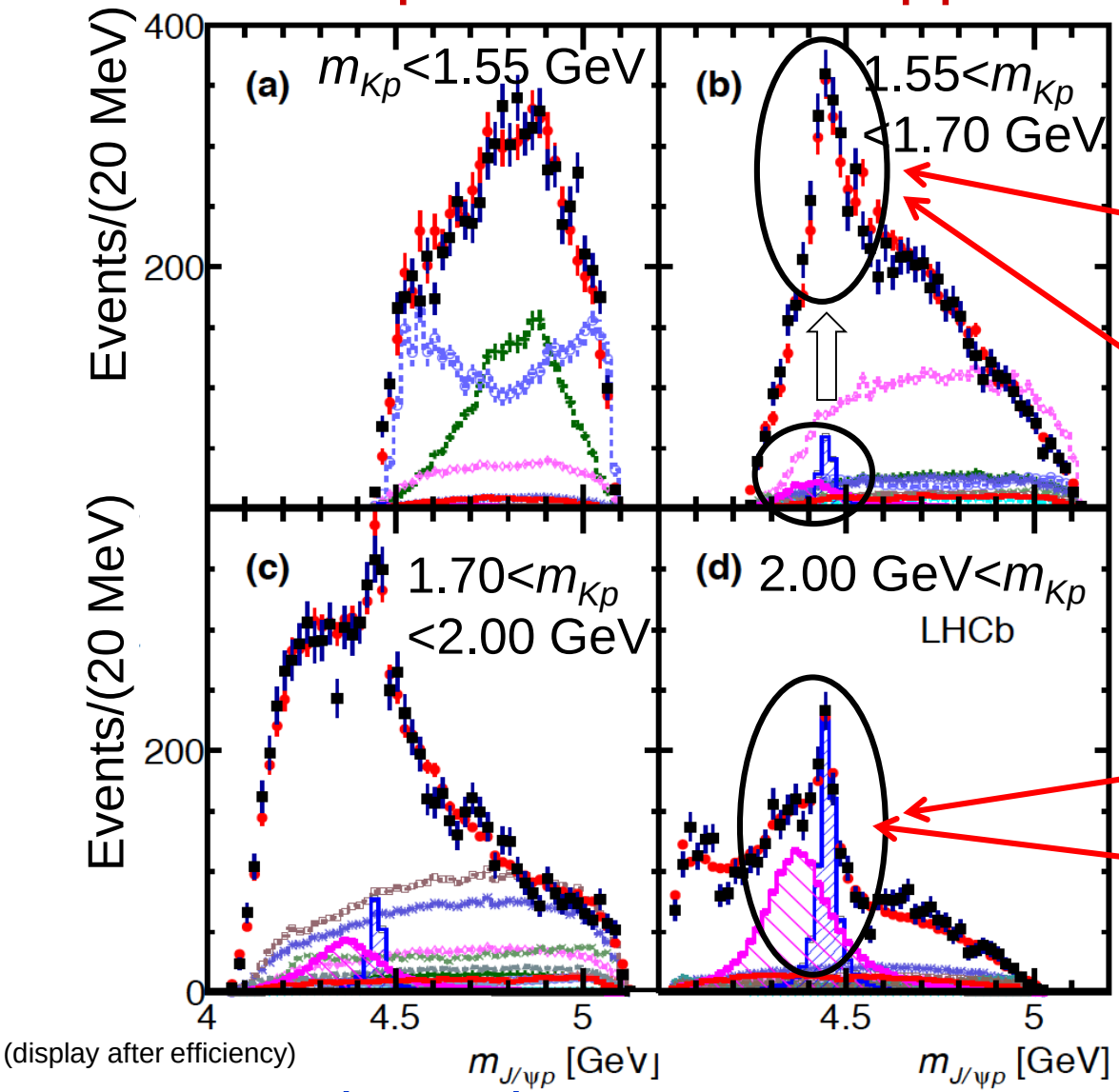

(display after efficiency)

$P_c(4450)$
$P_c(4380)$

Positive interference between the P_c states

(display before efficiency)

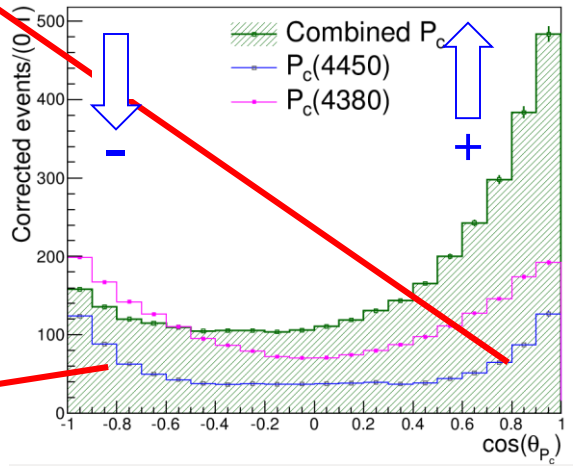

Negative interference between the P_c states

- Two opposite parity states necessary to generate the interference pattern

Results

- Parameters of the P_c^+ states:

State	Mass (MeV)	Width (MeV)	Fit fraction (%)
$P_c(4380)^+$	**4380 ± 8 ± 29**	**205 ± 18 ± 86**	**8.4 ± 0.7 ± 4.2**
$P_c(4450)^+$	**4449.8 ± 1.7 ± 2.5**	**39 ± 5 ± 19**	**4.1 ± 0.5 ± 1.1**

- With the $\mathcal{B}(\Lambda_b^0 \to J/\psi\, p\, K^-)$ measurement (arXiv:1509.00292) we can also calculate the branching fractions:

$$\mathcal{B}(\Lambda_b^0 \to P_c^+ K^-)\mathcal{B}(P_c^+ \to J/\psi p) = \begin{cases} (2.56 \pm 0.22 \pm 1.28^{+0.46}_{-0.36}) \times 10^{-5} & \text{for} \quad P_c(4380)^+ \\ (1.25 \pm 0.15 \pm 0.33^{+0.22}_{-0.18}) \times 10^{-5} & \text{for} \quad P_c(4450)^+ \end{cases}$$

Resonance Phase Motion

- Relativistic Breit-Wigner function is used to model resonances

$$BW(m|M_0,\Gamma_0) = \frac{1}{M_0^2 - m^2 - iM_0\Gamma(m)} \quad , \qquad \Gamma(m) = \Gamma_0 \left(\frac{q}{q_0}\right)^{2L+1} \frac{M_0}{m} B'_L(q,q_0,d)^2$$

- The complex function $BW(m|M_0,\Gamma_0)$ displayed in an Argand diagram exhibits a circular trajectory.

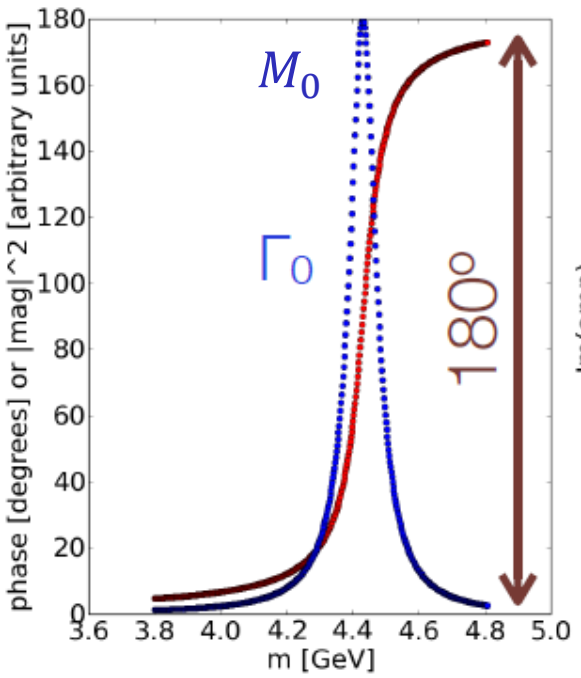

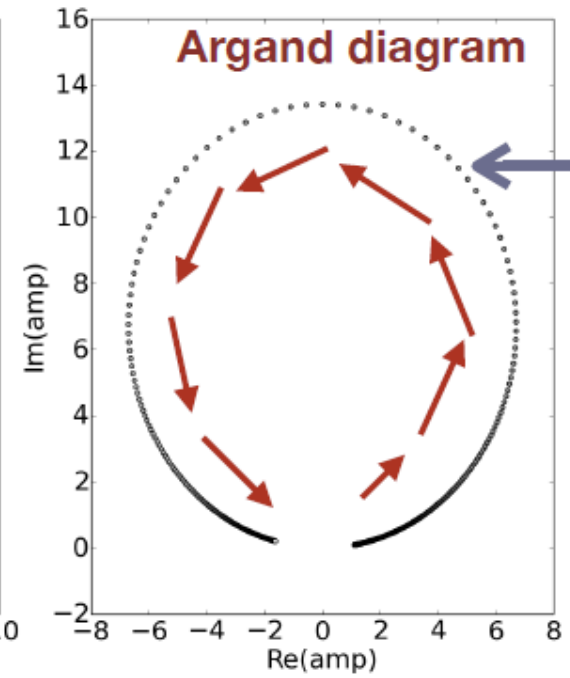

- Circular trajectory in complex plane is characteristic of resonance
- Circle can be rotated by arbitrary phase
- Phase change of 180° across the pole

Resonance Phase Motion

- The Breit-Wigner shape for individual P_c's is replaced with 6 independent amplitudes in $M_0 \pm \Gamma_0$
- $P_c(4450)$: shows resonance behavior: a rapid counter-clockwise change of phase across the pole mass
- $P_c(4380)$: does show large phase change, but is not conclusive.

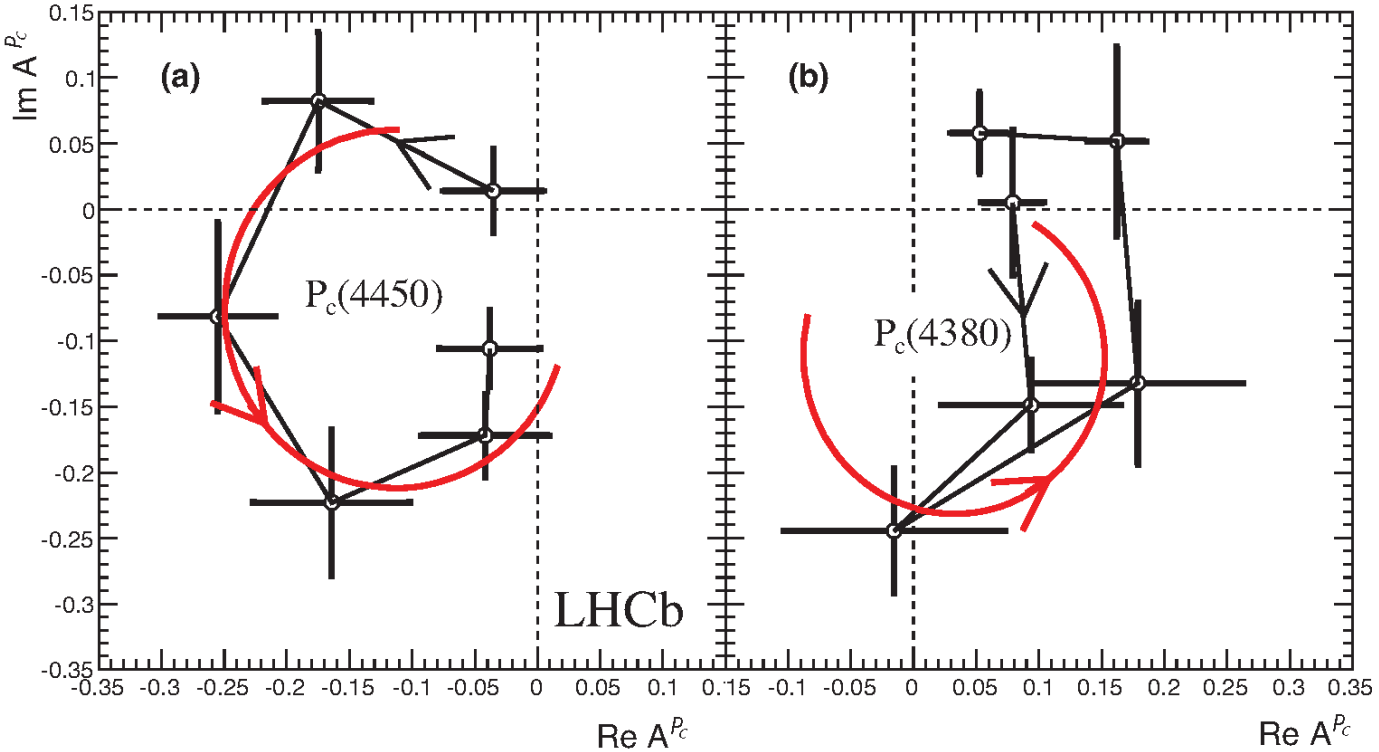

Plot fitted values for amplitudes in an Argand diagram

Breit-Wigner Prediction

Fitted Values

Interpretations of the states

diquarks

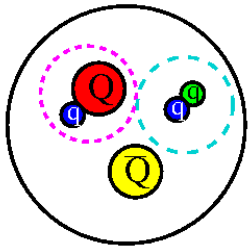

molecular

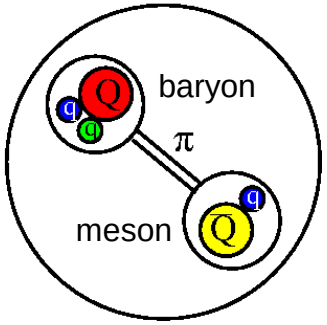

triquark

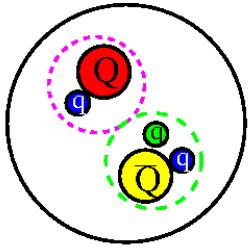

- Already a lot of activity on interpreting these states, with a variety of models being proposed.
- Most common models employ molecular binding or additional hadron building blocks of diquarks or triquarks.
- Additional explanations have been offered in terms of kinematical effects. However these cannot explain two states.

Where else to look for these pentaquarks?

- There are many ideas on where to look. None will be as ideal as the clean J/ψ signature plus two charged tracks forming a secondary vertex. This was a good channel to accidentally find this in.
- They can be looked for in decays to other charmonium states: $\eta_c p$, $\chi_c p$
- Or to open charm pairs: $\Lambda_c \overline{D}, \Lambda_c \overline{D^*}, \Sigma_c \overline{D}$
- Would be very interesting to see them from different sources:
  - Direct production: However there is a difficulty from huge number of protons coming from primary vertices
  - It's been proposed to look for these states in $\gamma p \to J/\psi\, p$

Conclusions

- Two pentaquark candidates decaying to J/ψp have been observed with overwhelming significance in a state of the art amplitude analysis. Both are absolutely needed to obtain a good description of the data.

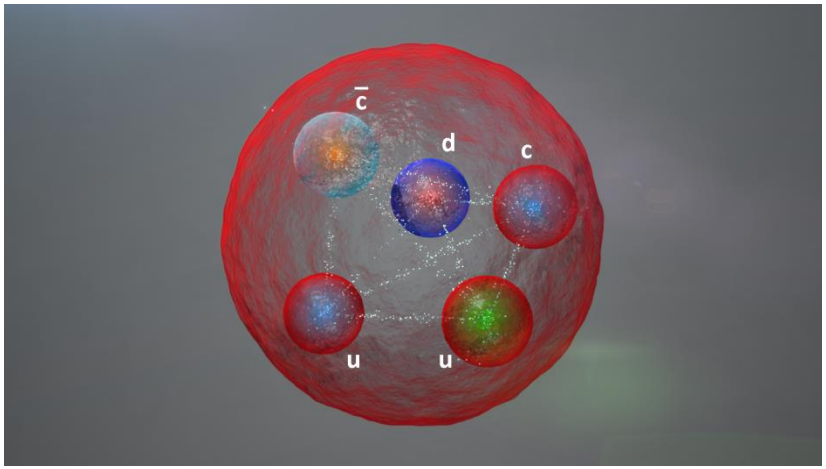

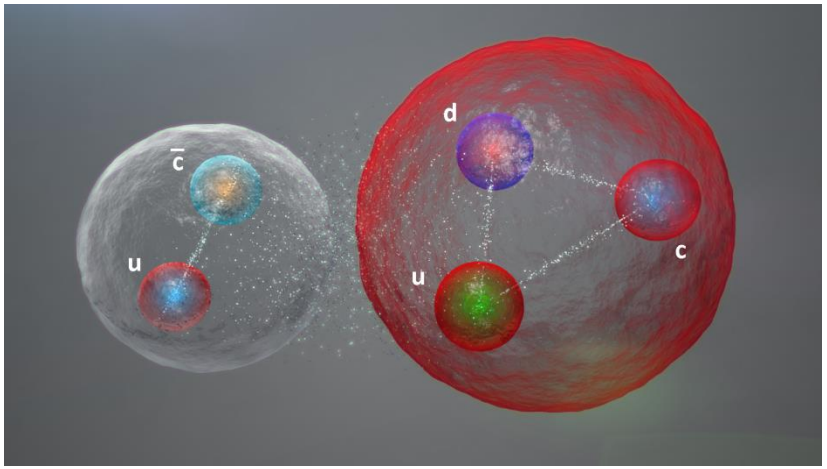

- The nature of the states is unknown. For elucidation, more sensitive studies as well as searches for other pentaquark candidates will be absolutely necessary.
- Towards this effort we continue to fully utilize the Run 1 data, and have increased statistics on the way. LHCb expects 8 fb^{-1} in Run 2 (-2018) followed by the detector/luminosity upgrade which will bring ~50 fb^{-1} by 2028.
- We look forward to more input from theory and other experiments.

BACKUP SLIDES

$\Lambda_b^0 \rightarrow J/\psi$ p K^- Selection

- The data sample consists of the full LHCb Run 1 data set of $3fb^{-1}$
- Candidates have a $(\mu^+\mu^-)Kp$ vertex, with the $(\mu^+\mu^-)$ pair consistent with a J/ψ

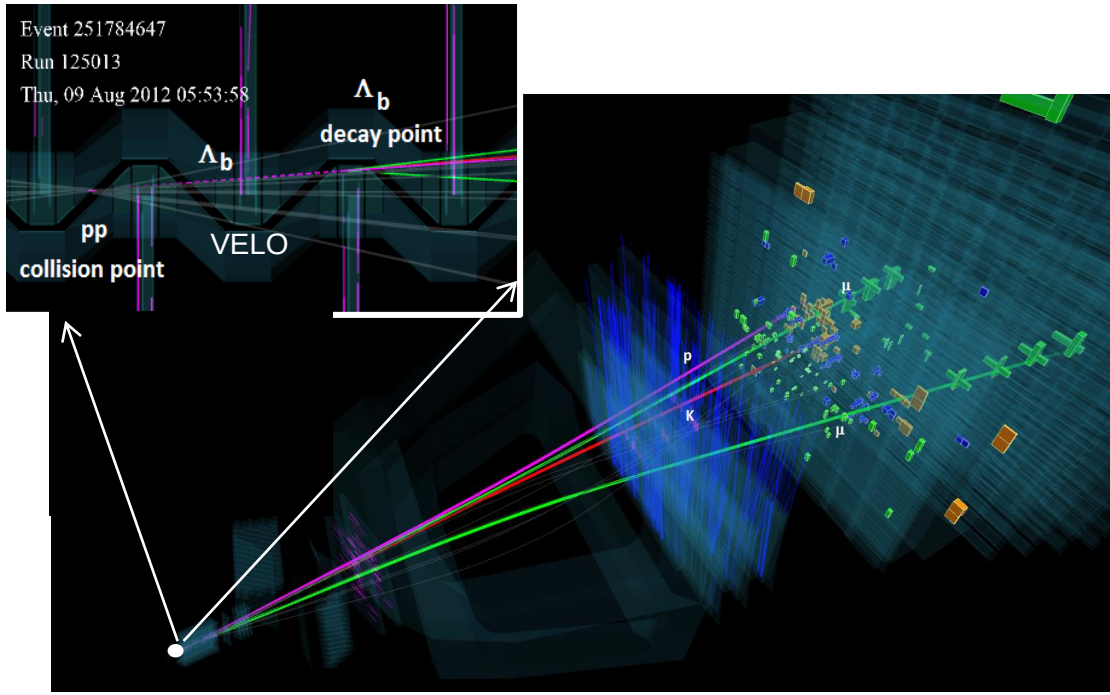

- Standard selection to ensure good track and vertex quality, as well as cuts on particle identification, p_T cuts, and separation from the primary vertex.
- Reflections from B^0 and B_s are vetoed.
- Final background suppression is done with a multivariate analyzer (boosted decision tree).

Λ^* Matrix Element

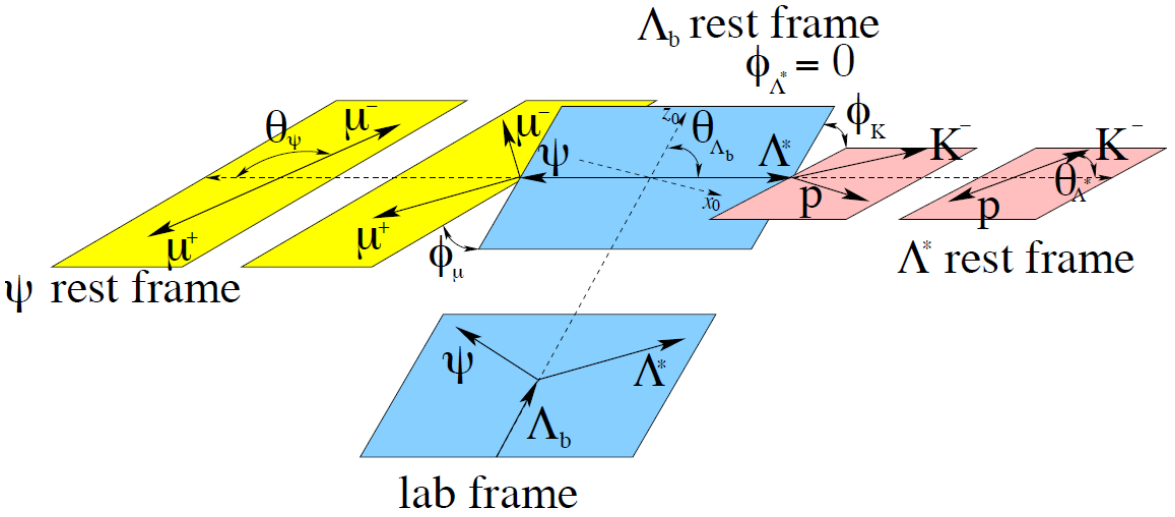

Completely describes the decay $\Lambda_b \to \Lambda^* J/\psi$ with $\Lambda^* \to Kp$ and $J/\psi \to \mu\mu$

4-6 independent **complex** helicity couplings per Λ_n^* resonance

6 independent data variables:
1 mass, 5 angles

$$\mathcal{M}^{\Lambda^*}_{\lambda_{\Lambda_b^0}, \lambda_p, \Delta\lambda_\mu} \equiv \sum_n \sum_{\lambda_{\Lambda^*}} \sum_{\lambda_\psi} \mathcal{H}^{\Lambda_b^0 \to \Lambda_n^* \psi}_{\lambda_{\Lambda^*}, \lambda_\psi} D^{\frac{1}{2}}_{\lambda_{\Lambda_b^0}, \lambda_{\Lambda^*} - \lambda_\psi}(0, \theta_{\Lambda_b^0}, 0)^* \mathcal{H}^{\Lambda_n^* \to Kp}_{\lambda_p, 0} D^{J_{\Lambda_n^*}}_{\lambda_{\Lambda^*}, \lambda_p}(\phi_K, \theta_{\Lambda^*}, 0)^* R_n(m_{Kp}) D^1_{\lambda_\psi, \Delta\lambda_\mu}(\phi_\mu, \theta_\psi, 0)^*$$

$$R_X(m) = B'_{L_X^{\Lambda_b^0}}(p, p_0, d) \left(\frac{p}{M_{\Lambda_b^0}}\right)^{L_{\Lambda_b^0}^X} \mathrm{BW}(m|M_{0X}, \Gamma_{0X})\, B'_{L_X}(q, q_0, d) \left(\frac{q}{M_{0X}}\right)^{L_X}$$

$$\mathrm{BW}(m|M_{0X}, \Gamma_{0X}) = \frac{1}{{M_{0X}}^2 - m^2 - iM_{0X}\Gamma(m)}$$

Blatt-Weisskopf functions

Breit-Wigner

P_c^+ Matrix Element

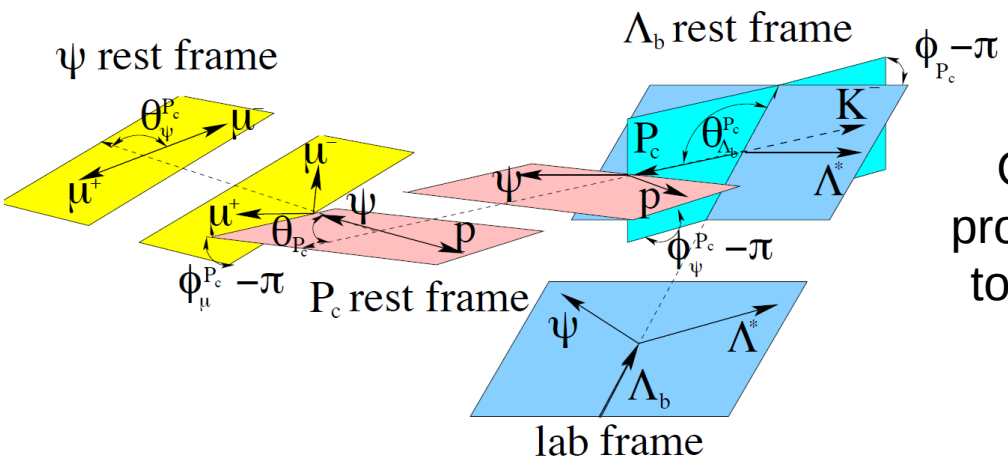

Completely describes the decay
$\Lambda_b \to P_c K$ with $P_c \to J/\psi\, p$ and $J/\psi \to \mu\mu$

One more angle than in Λ^* decay: P_c^+ production angles must be defined relative to the Λ_b reference frame established for $\Lambda_b \to J/\psi \Lambda^*$ decay

1 mass ($m_{J/\psi p}$), 6 angles
all derivable from the Λ^* decay variables

3-4 independent **complex** helicity couplings per P_{cj}^+ resonance depending on its J^P

$$\mathcal{M}^{P_c}_{\lambda_{\Lambda_b^0},\lambda_p^{P_c},\Delta\lambda_\mu^{P_c}} \equiv \sum_j \sum_{\lambda_{P_c}} \sum_{\lambda_\psi^{P_c}} \mathcal{H}^{\Lambda_b^0 \to P_{cj} K}_{\lambda_{P_c},0} D^{\frac{1}{2}}_{\lambda_{\Lambda_b^0},\lambda_{P_c}}(\phi_{P_c},\theta^{P_c}_{\Lambda_b^0},0)^*$$

$$\mathcal{H}^{P_{cj}\to\psi p}_{\lambda_\psi^{P_c},\lambda_p^{P_c}} D^{J_{P_{cj}}}_{\lambda_{P_c},\lambda_\psi^{P_c}-\lambda_p^{P_c}}(\phi_\psi,\theta_{P_c},0)^* R_{P_{cj}}(m_{\psi p})\; D^{1}_{\lambda_\psi^{P_c},\Delta\lambda_\mu^{P_c}}(\phi_\mu^{P_c},\theta_\psi^{P_c},0)^*$$

$$R_X(m) = B'_{L^X_{\Lambda_b^0}}(p,p_0,d)\left(\frac{p}{M_{\Lambda_b^0}}\right)^{L^X_{\Lambda_b^0}} \mathrm{BW}(m|M_{0X},\Gamma_{0X})\, B'_{L_X}(q,q_0,d)\left(\frac{q}{M_{0X}}\right)^{L_X}$$

Blatt-Weisskopf functions

$$\mathrm{BW}(m|M_{0X},\Gamma_{0X}) = \frac{1}{{M_{0X}}^2 - m^2 - iM_{0X}\Gamma(m)}$$

Breit-Wigner

Λ^* Plus P_c^+ Matrix Element

- To add the two matrix elements together we need two additional angles to align the muon and proton helicity frames between the Λ^* and P_c decay chains.
  - This is necessary to describe Λ^* plus P_c^+ interferences properly

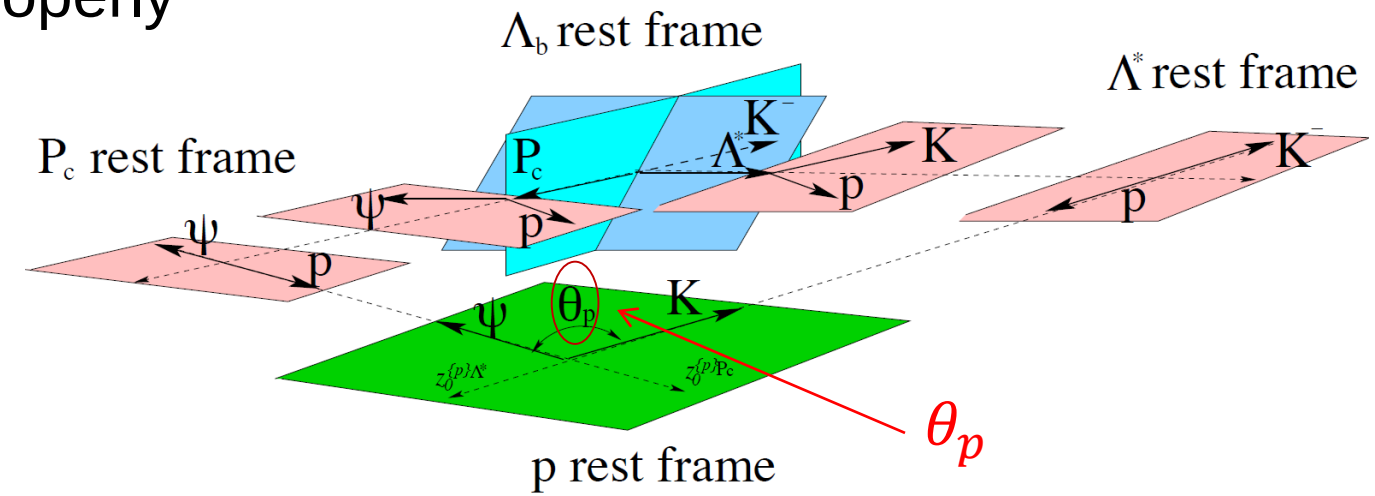

- With θ_p, α_μ the full matrix element is written as

$$|\mathcal{M}|^2 = \sum_{\lambda_{\Lambda_b^0}} \sum_{\lambda_p} \sum_{\Delta\lambda_\mu} \left| \mathcal{M}^{\Lambda^*}_{\lambda_{\Lambda_b^0}, \lambda_p, \Delta\lambda_\mu} + e^{i\,\Delta\lambda_\mu \alpha_\mu} \sum_{\lambda_p^{P_c}} d^{\frac{1}{2}}_{\lambda_p^{P_c}, \lambda_p}(\theta_p)\, \mathcal{M}^{P_c}_{\lambda_{\Lambda_b^0}, \lambda_p^{P_c}, \Delta\lambda_\mu} \right|^2$$

No need for exotic $J/\psi K^-$ contributions

- No evidence seen for a resonance in the Dalitz plane
- $J/\psi K^-$ system is well described by the Λ^* and P_c^+ reflections.

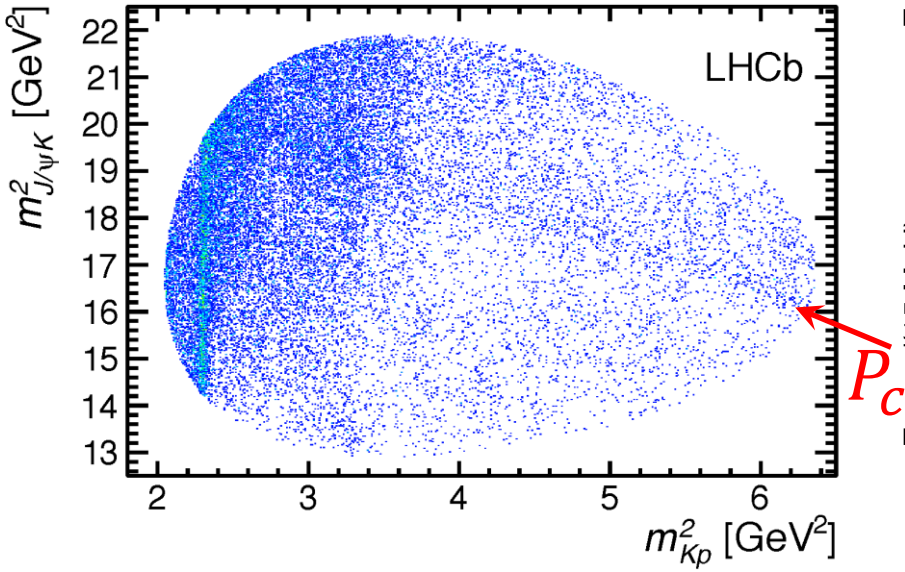

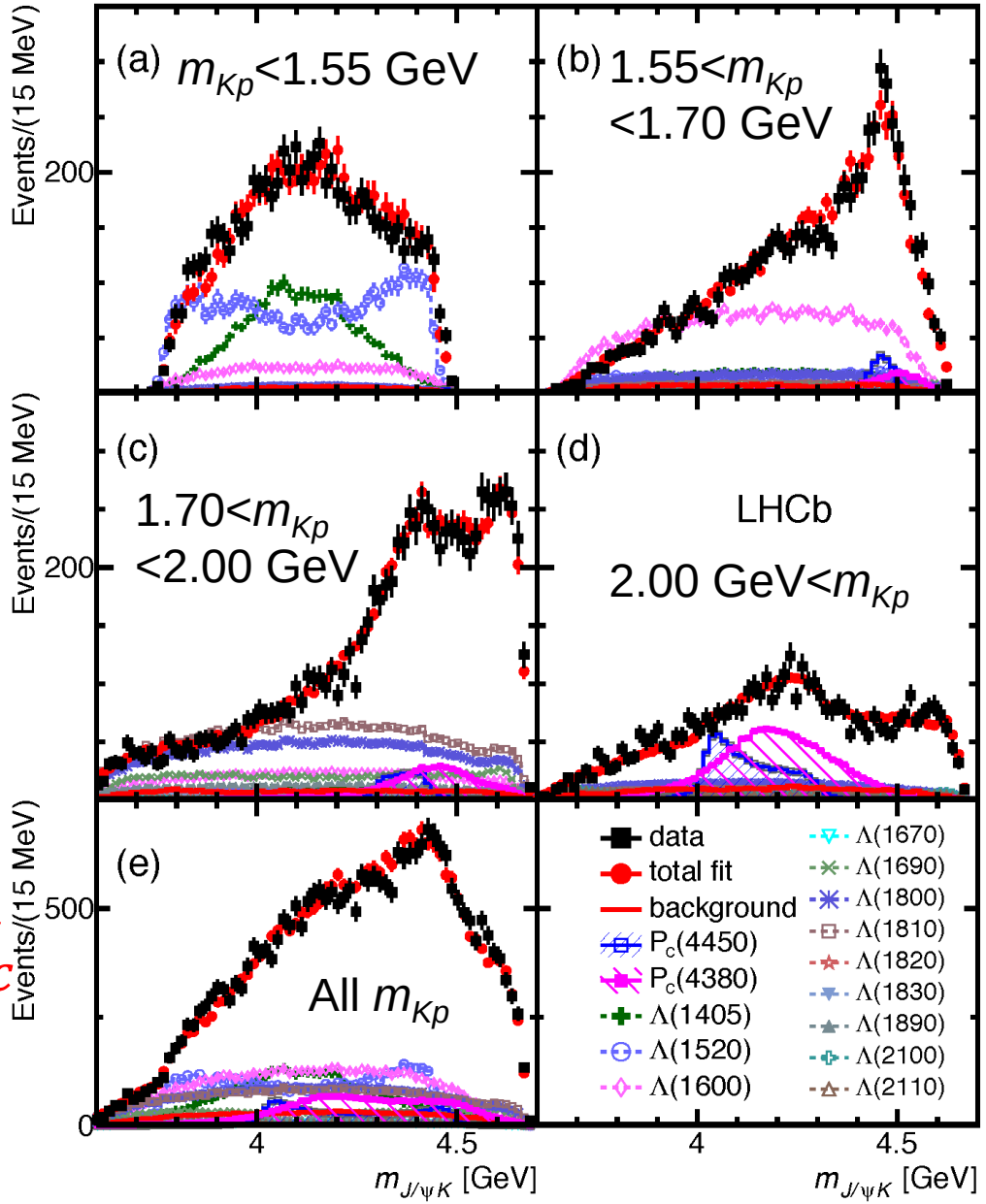

Systematic uncertainties

Source	M_0 (MeV)		Γ_0 (MeV)		Fit fractions (%)			
	low	high	low	high	low	high	$\Lambda(1405)$	$\Lambda(1520)$
Extended vs. reduced	21	0.2	54	10	3.14	0.32	1.37	0.15
Λ^* masses & widths	7	0.7	20	4	0.58	0.37	2.49	2.45
Proton ID	2	0.3	1	2	0.27	0.14	0.20	0.05
$10 < p_p < 100$ GeV	0	1.2	1	1	0.09	0.03	0.31	0.01
Nonresonant	3	0.3	34	2	2.35	0.13	3.28	0.39
Separate sidebands	0	0	5	0	0.24	0.14	0.02	0.03
J^P $(3/2^+, 5/2^-)$ or $(5/2^+, 3/2^-)$	10	1.2	34	10	0.76	0.44		
$d = 1.5 - 4.5$ GeV^{-1}	9	0.6	19	3	0.29	0.42	0.36	1.91
$L^{P_c}_{\Lambda_b^0}$ $\Lambda_b^0 \to P_c^+$ (low/high)K^-	6	0.7	4	8	0.37	0.16		
L_{P_c} P_c^+ (low/high) $\to J/\psi p$	4	0.4	31	7	0.63	0.37		
$L^{\Lambda_n^*}_{\Lambda_b^0}$ $\Lambda_b^0 \to J/\psi \Lambda^*$	11	0.3	20	2	0.81	0.53	3.34	2.31
Efficiencies	1	0.4	4	0	0.13	0.02	0.26	0.23
Change $\Lambda(1405)$ coupling	0	0	0	0	0	0	1.90	0
Overall	29	2.5	86	19	4.21	1.05	5.82	3.89
sFit/cFit cross check	5	1.0	11	3	0.46	0.01	0.45	0.13

- Uncertainties in the Λ^* model dominate
- Quantum number assignment and resonance parametrization are also sizeable.

Significances

- Significances assessed using the extended model.
- This includes the dominant systematic uncertainties, coming from difference between extended and reduced Λ^* model results.
- Fit quality improves greatly, and simulations of pseudoexperiments are used to turn the $\Delta(-2\ln\mathcal{L})$ values to significances

	$\Delta(-2\ln\mathcal{L})$	Significance
$0 \to 1\ P_c$	14.7^2	12σ
$1 \to 2\ P_c$	11.6^2	9σ
$0 \to 2\ P_c$	18.7^2	15σ

- Each of the states is overwhelmingly significant.

Complete set of fit fractions

Table 3: Fit fractions of the different components from cFit and sFit for the default $(3/2^-, 5/2^+)$ model. Uncertainties are statistical only.

Particle	Fit fraction (%) cFit	Fit fraction (%) sFit
$P_c(4380)^+$	8.42 ± 0.68	7.96 ± 0.67
$P_c(4450)^+$	4.09 ± 0.48	4.10 ± 0.45
$\Lambda(1405)$	14.64 ± 0.72	14.19 ± 0.67
$\Lambda(1520)$	18.93 ± 0.52	19.06 ± 0.47
$\Lambda(1600)$	23.50 ± 1.48	24.42 ± 1.36
$\Lambda(1670)$	1.47 ± 0.49	1.53 ± 0.50
$\Lambda(1690)$	8.66 ± 0.90	8.60 ± 0.85
$\Lambda(1800)$	18.21 ± 2.27	16.97 ± 2.20
$\Lambda(1810)$	17.88 ± 2.11	17.29 ± 1.85
$\Lambda(1820)$	2.32 ± 0.69	2.32 ± 0.65
$\Lambda(1830)$	1.76 ± 0.58	2.00 ± 0.53
$\Lambda(1890)$	3.96 ± 0.43	3.97 ± 0.38
$\Lambda(2100)$	1.65 ± 0.29	1.94 ± 0.28
$\Lambda(2110)$	1.62 ± 0.32	1.44 ± 0.28

Extended Model with Two P_c Resonances